arXiv:1610.00696v1 [cs.LG] 3 Oct 2016

Deep Visual Foresight for Planning Robot Motion

Chelsea Finn[1,2] and Sergey Levine[1,2]

***Abstract*— A key challenge in scaling up robot learning to many skills and environments is removing the need for human supervision, so that robots can collect their own data and improve their own performance without being limited by the cost of requesting human feedback. Model-based reinforcement learning holds the promise of enabling an agent to learn to predict the effects of its actions, which could provide flexible predictive models for a wide range of tasks and environments, without detailed human supervision. We develop a method for combining deep action-conditioned video prediction models with model-predictive control that uses entirely unlabeled training data. Our approach does not require a calibrated camera, an instrumented training set-up, nor precise sensing and actuation. Our results show that our method enables a real robot to perform nonprehensile manipulation – pushing objects – and can handle novel objects not seen during training.**

I. Introduction

Most standard robotic manipulation systems consist of a series of modular components for perception and prediction that can be used to plan actions for handling objects. Imagine that a robot needs to push a cup of coffee across the table to give it to a human. This task might involve segmenting an observed point cloud into objects, fitting a 3D model to each object segment, executing a physics simulator using the estimated physical properties of the cup and, finally, choosing the actions which move the cup to the desired location. However, when robots encounter previously unseen objects in complex, unstructured environments, this pipelined model-based approach can break down when any one stage has a sufficiently large modeling error. In particular, errors early in the process cause compounding errors later in the process, which in turn can produce actions that are ineffective in the real world: even a small error in the estimated liquid content in the cup or the friction coefficient might cause the robot to push it too high above its center of mass, causing the contents to spill. This is the essence of the unstructured open world problem: when the robot has to deal with the variability of the real world, methods based on rigid hand-engineered processes tend to suffer at the hands of special cases, exceptions, and unmodeled effects.

Learning-based methods have shown remarkable effectiveness in handling complex, unstructured environments in passive computer vision tasks, such as image classification [1] and object detection [2], by co-adapting low and high-level feature representations. Such approaches have also been used to learn complex, task-specific policies [3], [4] or value functions [5], but require supervision in the form of a reward function which can be difficult to specify in robotic domains. Motivated by large-scale, unsupervised robotic learning, we consider the question of whether it is possible to replace the hand-engineered robotic manipulation pipeline with a single general-purpose, learned model that connects low-level perception with physical prediction.

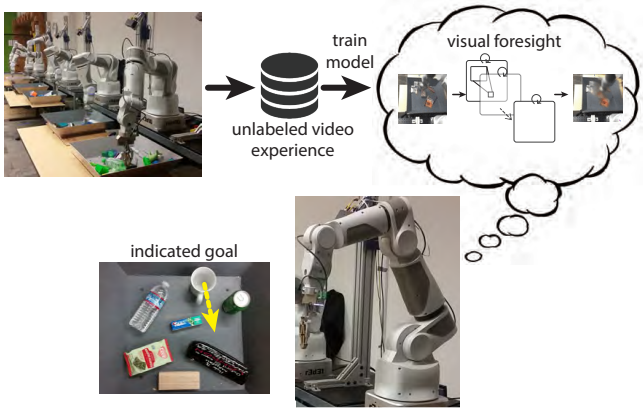

Fig. 1. Using our approach, a robot uses a learned predictive model of images, i.e. a visual imagination, to push objects to desired locations.

In this paper, we take a small step in the direction of this goal, by demonstrating an approach for combining a learned predictive model of raw sensory observations with model-predictive control (MPC). Unlike most methods for robotic learning, our approach requires minimal human involvement and can learn in an entirely self-supervised fashion, without a detailed reward function, an image of the goal, or ground truth object pose information. At test time, we define the task objective as moving a pixel or a group of pixels from their current position to a desired goal position (e.g. see Figure 1). This goal description allows us to specify how the robot should affect objects in its environment. Also at test time, our method optimizes for the sequence of actions that will move the pixels as desired. The actions are continuously replanned as the robot executes the task and receives new observations, allowing the method to correct for mispredictions.

The primary contribution of our paper is to demonstrate that deep predictive models of video can be used by real physical robotic systems to manipulate previously unseen objects. To that end, we present an MPC algorithm based on probabilistic inference through a learned predictive image model that allows a robot to plan for actions that move user-specified objects in the environment to user-defined locations. We apply a deep predictive model demonstrated on video prediction in prior work [6], and show how the

[1]Google Brain, Mountain View, CA
[2]Berkeley Artificial Intellgence Research (BAIR), Department of Electrical Engineering and Computer Science, University of California, Berkeley, Berkeley, CA 94720

ability of this model to learn implicit stochastic pixel flow can be leveraged within a probabilistic MPC framework. To evaluate the feasibility of robotic manipulation with learned video prediction models, we restrict the problem setting to nonprehensile pushing tasks. By planning through the model in real time, we show that it is possible to learn nonprehensile manipulation skills with fast visual feedback control in an entirely self-supervised setting, using only unlabeled training data and without camera calibration, 3D models, depth observations, or a physics simulator. Although the pushing tasks are relatively simple, the performance of our method suggests that the underlying predictive model learns a sufficiently detailed physical model of the world for basic manipulation. To the best of our knowledge, our work is the first instance of robotic manipulation using learned predictive video models with generalization to new, previously unseen objects.

II. Related Work

Standard model-based methods for robotic manipulation might involve estimating the physical properties of the environment, and then solving for the controls based on the known laws of physics [7], [8], [9]. This approach has been applied to a range of problems, including robotic pushing [10], [11], [12]. Despite the extensive work in this area, tasks like pushing an unknown object to a desired position remain a challenging robotic task, largely due to the difficulties in estimating and modeling the physical world [13]. Learning and optimization-based methods have been applied to various parts of the state-estimation problem, such as object recognition [14], pose registration [15], and dynamics learning [16]. However, estimating and simulating all of the details of the physical environment is exceedingly difficult, particularly for previously unseen objects, and is arguably unnecessary if the end goal is only to find the desired controls. For example, simple rules for adjusting motion, such as increasing force when an object is not moving fast enough, or the gaze heuristic [17], can be used to robustly perform visuomotor control without an over-complete representation of the physical world and complex simulation calculations. Our work represents an early step toward using learning to avoid the detailed and complex modeling associated with the fully model-based approach.

Several works have used deep neural networks to process images and represent policies for robotic control, initially for driving tasks [18], [19], later for robotic soccer [20], and most recently for robotic grasping [21], [22] and manipulation [4]. Although these model-free methods can learn highly specialized and proficient behaviors, they recover a task-specific policy rather than a flexible model that can be applied to a wide variety of different tasks. The high dimensionality of image observations presents a substantial challenge to model-based approaches, which have been most successful for low-dimensional non-visual tasks [23] such as helicopter control [24], locomotion [25], and robotic cutting [26]. Nevertheless, some works have considered modeling high-dimensional images for object interaction. For example, Boots et al. [27] learn a predictive model of RGB-D images of a robot arm moving in free space. Byravan et al. [28] learn a model similar to the one that we use here based on prior work [6], except that it predicts 3D rigid motions for constructing future depth images instead of pixel flow transformations for RGB images. These three works propose video prediction models, but do not demonstrate a method for using the learned model for control.

Agarwal et al. [29] learn an inverse model that can be used for poking objects, but do not demonstrate generalization to new objects, nor planning capabilities. Other works have used model-based approaches with a learned low-dimensional embedding of images [30], [31], [32], [33], defining the objective using an image of the goal; however, such methods have been demonstrated either on simple synthetic images, or without generalization to new objects. Our approach does not require an image of the goal and demonstrates generalization to new objects.

Our approach is related to visual servoing, which performs feedback control on features in an image [34], [35], [36] or the image pixels themselves [37]. Unlike visual servoing methods, our approach performs feedback control at the pixel level using a model learned entirely from unlabeled, real-world video data, without requiring any explicit camera calibration. As demonstrated in our experiments, our method can be used to move image pixels that are not directly actuated by the robot's joints – that is, perform nonprehensile manipulation. This is generally outside of the capability of standard model-based visual servoing techniques, due to the inherent discontinuities and complex, unknown dynamics.

III. Background

To perform visual model-predictive control, we use a deep predictive model of images trained on a large dataset of robotic pushing experience. In this section, we introduce notation and briefly describe the data collection process and model. Our dataset includes $50,000$ pushing attempts collected using 10 7-DoF arms, involving hundreds of objects.[1] During data collection, a bin containing between 10 and 20 objects is positioned in front of each robot, as shown in Figure 1. Each push attempt starts with the robot randomly selecting an initial pose along the outside border of the bin. Subsequently, the robot iteratively selects a new target gripper pose $\mathbf{a}_t$ and moves towards it. A new target pose is chosen at each time step $t \in \{0, \ldots, T\}$, where T is the episode length. The gripper pose is represented in the coordinate frame of the robot base as the positional coordinate in $3D$ and rotations pitch and yaw, while roll is kept constant. Thus, $\mathbf{a}_t$ is a vector of length 5. During data collection, the commanded poses are chosen randomly. The robot records sensor readings at 10 Hz, including the current gripper pose $\mathbf{x}_t$, the commanded gripper pose $\mathbf{a}_t$, and the RGB camera image of the workspace, I_t, and selects new commanded poses at 5 Hz.

[1]We have made the entire dataset publicly available for download at `http://sites.google.com/site/brainrobotdata`

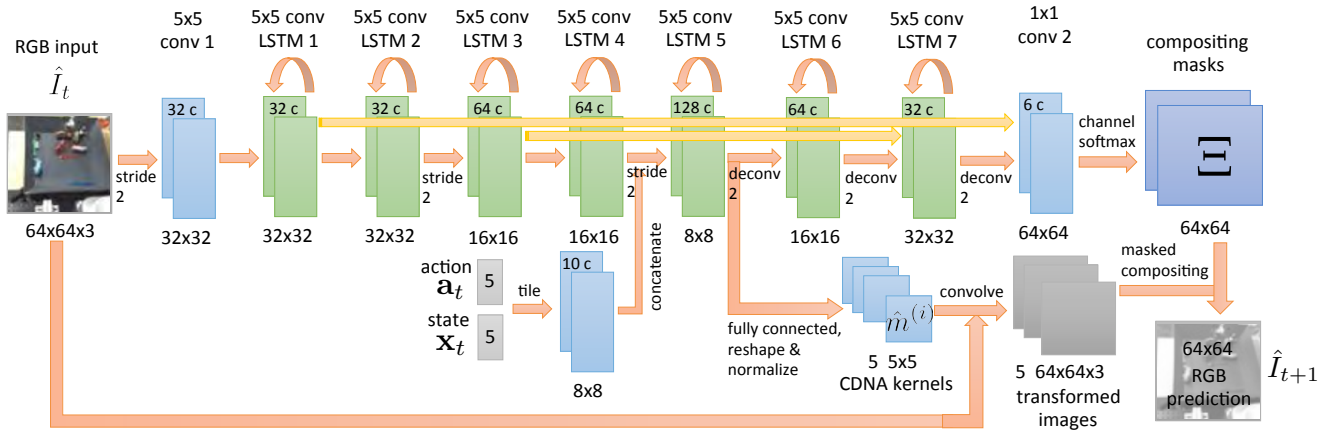

Fig. 2. Our video prediction model predicts stochastic pixel flow transformation from the current frame to the next frame, which allows it to generate predictions for subsequent images conditioned on a sequence of future actions. Predicted stochastic flow is parameterized by a set of normalized convolution filters that give rise to an independent Gaussian distribution over future images. Internally, our model predicts multiple stochastic flow channels, in order to process multiple separate moving objects. These channels are composited using learned object masks. The only supervision to the model consists of video, action, and state sequences, with no explicit supervision over flows or masks. The flows and masks therefore are an emergent property of the model, which we will exploit to perform visual MPC using high-level user commands. Further details about the model may be found in prior work [6].

The inputs to the predictive model $\mathcal{M}$ at each timestep consist of the current and previous images, which we will denote $I_{0:1}$ and the current and previous end-effector poses $\mathbf{x}_{0:1}$, as well as a sequence of future commands $\mathbf{a}_{1:H_p}$, where H_p is the prediction horizon used during training. Pairs of images and states are fed into the model to allow it to estimate the current velocities of moving objects. The model is trained to predict a distribution over the sequence of future image frames $I_{2:H_p+1}$ that result from executing the actions $\mathbf{a}_{1:H_p}$. However, since the full posterior over images is extremely high dimensional, we use a relatively simple factorization where each pixel is drawn from an independent Gaussian distribution. Although this assumption is simplistic, it is a common simplification in video and image generation models [38], [39]. The model is trained with maximum likelihood, which results in a mean squared error objective. We can therefore express the model probabilistically as $p_{\mathcal{M}}(I_{2:H_p}|I_{0:1},\mathbf{x}_{0:1},\mathbf{a}_{1:H_p})$.

As shown in Figure 2, the model uses a convolutional LSTM to predict the images. As an intermediate step, the model outputs a probabilistic flow map at each time step t, which we denote $\hat{F}_t$, that describes a linear transition operator that can be applied to each pixel in the preceding image. Intuitively, we expect different objects in different regions of the image to be moving in different ways. The model uses a set of normalized convolution kernels $\{m_c\}$ to capture the motion of object c by providing a distribution over nearby pixel locations at the next timestep. These object motion predictions are combined using masks $\{\Xi_c\}$ which specify the positions of the objects. The flow map $\hat{F}_t(x,y,k,l)$ denotes the probability of pixel (k,l) at time $t+1$ originating from location (x,y) at time t, and is given by the following.

$$\hat{F}_t(x,y,k,l) = \sum_c \Xi_{c,t}(x,y)\hat{m}_{c,t}(k,l)$$

The model can then output a prediction for the mean of the distribution over the next image, which we denote $\hat{I}_{t+1}$, according to the following equation:

$$\hat{I}_{t+1}(x,y) = \sum_{k\in(-\kappa,\kappa)}\sum_{l\in(-\kappa,\kappa)} \hat{F}_t(x,y,k,l)\hat{I}_t(x-k,y-l)$$

Note that this equation is an untied convolution operation between the filters $\hat{F}_t$ and the image $\hat{I}_t$, since the filters are different for each pixel location (x,y). The operator $\hat{F}_t$ can also be seen as the transition operator in a Markov chain. We will use $\hat{I}_{t+1} = \hat{F}_t \odot I_t$ to denote the application of the flow operator. Since this operator is linear, the distribution over a subsequent image can be obtained simply by transforming the mean of the distribution over the current image. The predicted image mean $\hat{I}_{t+1}$ is fed back into the network recursively to generate the next flow and image in the sequence. Note that no explicit flow supervision is provided to the network: training uses only the raw image pixels for supervision. The stochastic flow maps are an implicit, emergent property of the model, but one that will prove useful in visual MPC, as we will discuss in the following section. For convenience, we will use $\mathcal{M}(I_{t-1:t},\mathbf{x}_{t-1:t},\mathbf{a}_{t:H}) = \hat{F}_{t:H}$ to denote the function that uses the learned model to output a sequence of flows conditioned on pairs of images and states, as well as a sequence of future actions, for some horizon H. We can therefore define the predicted image distribution as

$$\begin{aligned} p_{\mathcal{M}}(I_{t+1}|I_{t-1:t},\mathbf{x}_{t-1:t},\mathbf{a}_t) &= \mathcal{N}(\hat{F}_t \odot I_t, \sigma^2\mathbf{I}) \\ &= \mathcal{N}(\mathcal{M}(I_{t-1:t},\mathbf{x}_{t-1:t},\mathbf{a}_t)\odot I_t, \sigma^2\mathbf{I}), \end{aligned}$$

where $\sigma^2\mathbf{I}$ is a constant diagonal covariance. Predictions for subsequent images I_{t+k} can then be made recursively, with mean given by $\mathcal{M}(I_{t-1:t},\mathbf{x}_{t-1:t},\mathbf{a}_{t:t+k-1})\circ\hat{I}_{t+k-1}$.

We use the same network architecture as in prior work [6], except for the addition of layer normalization [40] after each layer for more robust training, and the use of 5 masks instead of 10 for slightly faster computation.

IV. Visual MPC with Learned Video Prediction Models

At test time, our system receives a high level goal from the user, which we discuss in Section IV-A, and then uses model-predictive control (MPC) together with our deep video prediction model to choose controls that will realize the user's commanded goal, as shown in Figure 1. Because video prediction models do not explicitly model objects, we cannot represent the task goal using standard notions of object poses. In this section, we outline exactly how the objective is specified and represented, and how to probabilistically evaluate candidate actions using the model and goal representation. Lastly, in Section IV-C, we present our method for planning and replanning actions using MPC, which involves rolling out the video prediction model H timesteps into the future. We show the full algorithm in Algorithm 1, which combines the learned model, the high-level goal specification, and MPC to probabilistically plan future actions.

A. Specifying Goals with Pixel Motion

To plan with a predictive model of images, we need a way to specify task objectives that can be automatically evaluated for each of the model's predicted visual futures. In this work, the goal is specified by the user in terms of pixel motion. Intuitively, the user specifies a pixel in the image and tells the robot where that pixel should be moved to. The user selects one or more desired source pixels in the initial image, which we will denote $d_0^{(1)}, \ldots, d_0^{(P)}$, with each pixel's position given by $(x_d^{(i)}, y_d^{(i)})$, and then specifies a corresponding goal position for each of those pixels, which we will denote $g^{(1)}, \ldots, g^{(P)}$, with each goal position given by $(x_g^{(i)}, y_g^{(i)})$. With this goal specification, the robot can plan to move the objects for which the selected pixels belong. This kind of goal specification is quite general and can be used to command arbitrary rearrangements of objects, such as clearing a table. In a practical application, the commands themselves could be issued either directly by a human user selecting points in an image, or by a higher-level planning process. This goal representation is easy to specify, does not require instrumentation of the environment e.g. via motion capture or AR markers, and can represent a variety of object manipulation tasks. Unlike most approaches to robotic manipulation, it also does not use or need an explicit representation of objects. Example pixel motion goals are shown in Figure 5.

B. Evaluating Actions with Implicit Pixel Advection

Here, we describe how our method evaluates a proposed action sequence using probabilistic inference under the learned predictive model $\mathcal{M}$. For simplicity, first consider the goal of moving a single designated pixel $d_0 = (x_d, y_d)$ in the initial image to a goal position $g = (x_g, y_g)$. We need to evaluate the probability of achieving this goal under the model $\mathcal{M}$ for a given initial image I_t, intial state $\mathbf{x}_t$, and sequence of H future actions $\mathbf{a}_t, \ldots, \mathbf{a}_{t+H}$. As described in Section III, our video prediction model predicts stochastic flow operators $\hat{F}_{t+k}$ at each time step, which can be used to transform prior images or independent Gaussian pixel distributions into independent Gaussian pixel distributions for the next image, according to $\hat{I}_{t+k} = \hat{F}_{t+k} \odot \hat{I}_{t+k-1}$. We can also use these stochastic flow operators to predict how individual pixels will move, conditioned on a sequence of actions. Since the flow operators are stochastic, they provide a distribution over pixel motion conditioned on the actions. This suggests a natural approach to planning using maximum likelihood: determine the sequence of actions that maximizes the probability of the designated pixel moving to the goal position.

Formally, we construct an initial probability distribution over the designated pixel's position at the current time step t, which we denote $P(s_t)$. We assume that the current position of the designated pixel $d_t = (x_d, y_d)$ is known at time t, as it is provided by a user at time $t = 0$ can be tracked thereafter. Thus, we define the distribution at the current time step t as

$$P(s_t) = \begin{cases} 1 \text{ if } s_t = d_t \\ 0 \text{ otherwise} \end{cases}$$

Our goal is to compute the distribution over the designated pixel's position at the end of the MPC horizon, denoted $P(s_H | I_{t-1:t}, \mathbf{x}_{t-1:t}, \mathbf{a}_{t:t+H}, d_t)$, and choose the actions that maximize the probability $P(s_H = g | I_{t-1:t}, \mathbf{x}_{t-1:t}, \mathbf{a}_{t:t+H}, d_t)$. This corresponds to probabilistic inference over the action sequence $\mathbf{a}_{t:t+H}$. Recall that our predictive model outputs a stochastic flow operator $\hat{F}_t$ at each time step. The stochastic flow corresponds to a stochastic transition operator over the pixel positions, and we can therefore propagate the distribution over the designated pixel forward in time using $\hat{F}_t$. Let $\mathbf{P}_{t+k}$ denote the 2D conditional distribution $P(s_{t+k} | I_{t-1:t}, \mathbf{x}_{t-1:t}, \mathbf{a}_{t:t+k}, d_t)$, we then have:

$$\begin{aligned} \mathbf{P}_{t+k+1} &= \hat{F}_{t+k} \odot \mathbf{P}_{t+k} \\ &= \mathcal{M}(I_{t-1:t}, \mathbf{x}_{t-1:t}, \mathbf{a}_{t:t+k}) \odot \mathbf{P}_{t+k}. \end{aligned} \tag{1}$$

Applying this computation recursively for H steps, we obtain $\mathbf{P}_{t+H} = P(s_{t+H} | I_{t-1:t}, \mathbf{x}_{t-1:t}, \mathbf{a}_{t:t+H}, d_t)$, which describes the probability distribution over the position of the designated pixel at the end of the MPC horizon. The probability of successfully moving the designated pixel to the goal location is then given simply by $\mathbf{P}_{t+H}(g)$. This process can easily be extended to multiple pixels by computing the probability of success for each pixel separately, and summing the log-probabilities.

Interestingly, this process makes use of the model's implicit flow predictions, instead of the predicted images themselves. However, the ability of the model to predict images is what enables us to train it without explicit flow supervision.

C. Sampling-Based Model-Predictive Control with Deep Models

The goal of our MPC-based controller is to determine the sequence of actions that maximizes the probability of the designated pixel or pixels being moved to their corresponding goal locations. The previous section describes how we can evaluate a candidate action sequence $\mathbf{a}_{t:t+H}$ to

Algorithm 1 Visual MPC with Deep Predictive Models

inputs: predictive model $\mathcal{M}$, designated pixel $\{d_0\}$, pixel goal position $\{g\}$
for $t = 0...T$ **do**
  Initialize Q_1 with uniform distribution.
  for $j = 1...J_t$ **do**
    Sample M action sequences $\{\mathbf{a}_{t:t+H}^{(m)}\}$ from Q_j.
    Use model $\mathcal{M}$ to compute the distributions over future pixel locations $\mathbf{P}_{t+H}^{(m)}$ using Equation 1
    Fit multivariate Gaussian distribution Q_{j+1} to K samples with highest probability of success $\mathbf{P}_{t+H}^{(m)}$
  end for
  Execute action $\mathbf{a}_t^*$ with highest probability of success
  Observe new image I_{t+1}.
  Set next designated pixel location d_{t+1} using optical flow computed from image observations $I_{t:t+1}$, and d_t.
end for

determine the probability that it will move the designated pixel to the goal location, given by $\mathbf{P}_{t+H}(g) = P(s_{t+H} = g|I_{t-1:t}, \mathbf{x}_{t-1:t}, \mathbf{a}_{t:t+H}, d_t)$. In order to use this evaluation to choose the best actions, we perform an optimization over a short horizon of actions at each time step, using a stochastic optimization algorithm called the cross-entropy method (CEM) [41]. This procedure is outlined in Algorithm 1, and described next.

At each time step t, we sample M action sequences of length H, $\{\mathbf{a}_t^{(m)}, \ldots, \mathbf{a}_{t+H}^{(m)}\}$, and compute the probabilities of success for each one, denoted by $\mathbf{P}_{t+H}^{(m)}(g) = P(s_{t+H} = g|I_{t-1:t}, \mathbf{x}_{t-1:t}, \mathbf{a}_{t:t+H}^{(m)}, d_t)$. We then select the K action sequences with the highest values of $\mathbf{P}_{t+H}^{(m)}(g)$, fit a multivariate Gaussian distribution to these K selected action sequence, and resample a new set of M action sequences from this distribution. The new set of action sequences improves on the previous set, and the resampling and refitting process is repeated for J_t iterations. This corresponds to the CEM stochastic optimization algorithm. At the end of the last iteration, we take the sampled action sequence $\mathbf{a}_t^*, \ldots, \mathbf{a}_{t+H}^*$ that is most likely to be successful, and execute $\mathbf{a}_t^*$ on the robot. We use $J_t = 4$ iterations, $M = 40$ samples per iteration, and $K = 10$ samples during the initial planning phase ($t = 0$) and, when replanning in real-time ($t > 0$), we take $J_t = 1$ iteration of $M = 20$ samples, performing just one round of sampling. Note that each batch of M samples corresponds to a forward pass through deep recurrent network with a batch size of M, and therefore can be parallelized very efficiently.

After the first timestep, the designated pixel locations may have changed from their initial positions due to motion of the objects. To update the estimated position of each pixel, we compute optical flow on the previous and latest image observation, using the method of Anderson et al. [42], an optical flow algorithm used in a large-scale production system. For speed, the optical flow computation is done on the CPU while evaluating the model's video predictions in parallel using a GPU.

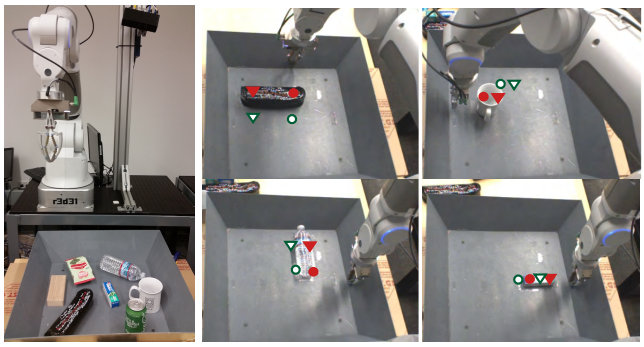

Fig. 3. The experimental setup is shown on the left, including the 7 test objects previously not seen in the training set. On the right, we show four of the ten pushing tasks in the quantitative evaluation. The red and green-outlined markers indicate the human-specified start and goal pixel locations, respectively.

V. Experiments

In our experimental evaluation, we aim to answer the following questions: (1) Can we use action-conditioned video prediction models to manipulate novel objects that were not previously seen during training? (2) Can video prediction models trained entirely on raw image pixels make meaningful and nontrivial inferences about the behavior of physical objects? To answer these questions, we conduct both qualitative and quantitative experiments, which we describe in the next sections. We aim to answer question (1) by evaluating our method on new objects not seen during training, and we answer question (2) through comparison to baseline methods that either move the arm to user-specified positions, or use optical flow to perform continuous replanning. We also answer question (2) through qualitative experiments aimed to construct physically nuanced pushing scenarios that require reasoning about rotations and centers of mass.

Note that the intent of our experiments is not to demonstrate that our approach provides the highest accuracy or performance for precise nonprehensile manipulation, but rather to demonstrate the flexibility of a data-driven, learning-based approach and illustrate that, even with no prior knowledge about objects, physics, or contacts, a predictive model trained entirely on raw video data can still infer characteristics of the physical world that are useful for robotic manipulation.

A. Experimental Setup

We use a 7-DoF robot arm to perform the pushing tasks in our experiments, with an RGB camera positioned over the shoulder, as shown in Figure 3. As discussed previously, the pushing task consists of episodes of length $T = 15$ where the goal is to move M pixels from their current locations $\{(x_s^{(i)}, y_s^{(i)})\}$ to corresponding goal locations $\{(x_g^{(i)}, y_g^{(i)})\}$. Unless otherwise specified, all objects in the experiments were not seen previously in the training set. A video of our experiments is available online.[2]

We use images with a resolution of 64×64 pixels and a planning horizon of $H = 3$, corresponding to about 800 ms.

[2]See https://sites.google.com/site/robotforesight/

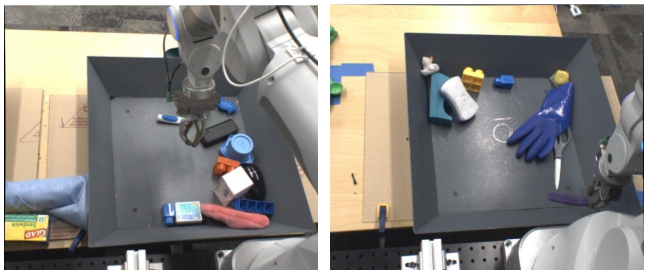

Fig. 4. The data for training the model was collected on 10 robots with varying camera angles and positions. These images show the camera angles for two of the robots used during data collection. Note the difference in the position of the robot base. Due to these variations, our video prediction model learns a calibration-invariant representation of object interactions.

This allows us to replan in real time, with new controls computed about every 200 ms. To reduce the dimensionality of the action space and further speed up inference, we tie the commanded action across time, such that the model is considering one commanded action, kept constant for H timesteps. Because of the short time horizon, we largely consider pushing tasks that involve fast, reactive control rather than long-term planning. All of the online model computations, including replanning, are done using a standard desktop computer and a single, commercially-availble GPU.

B. Quantitative Comparisons

We provide quantitative comparisons to three baselines, with the aim of evaluating whether or not our video prediction model has learned a meaningful and nontrivial notion of objects and physical interaction. Recall that object identity, inertia, and contact dynamics are not provided to nor encoded in the model explicitly, but must be learned entirely from data. Correspondingly, our baselines do not use any knowledge about the objects in the scene, but are reasonably effective for the short horizon pushing tasks that we consider. The baselines are as follows:

1) Select actions randomly from a uniform distribution.
2) Servo the end-effector to the goal pixel position (x_g, y_g), using a known camera calibration.
3) Servo the end-effector along the vector from the current pixel position $d_t = (x_t, y_t)$ to the goal (x_g, y_g), with continuous replanning based on the current pixel position estimated using optical flow.

If more than one designated pixel is specified, the last two baselines use the first pixel only. The first baseline of randomly selecting actions serves to calibrate the difficulty of the task in choosing effective actions. The last two baselines serve as a comparison to our method to test whether our model is learning something meaningful about physical object interaction, beyond simple motions of the arm. Note that the last two baselines require hand-to-camera calibration, which our model does not use. Since the data that was used for training our predictive model was collected on a variety of robots with varying camera placements and angles, as illustrated in Figure 4, our video prediction model was forced to learn a calibration-agnostic predictive strategy. The final baseline and our method use an optical flow solver [42] to track the position of the pixel for replanning. Note, however, that the predictive model itself does not use the optical flow to make predictions. The optical flow is used only during the replanning phase to provide the initial $P(s_t)$ distribution. The flow solver is also used to quantitatively evaluate the distance between the final position of the pixel and the goal position of the pixel.

Note that we specifically choose baseline methods that do not have prior knowledge about objects or physics. It is of course possible to design a model-based pushing algorithm that uses an object detector and physics simulator to more precisely localize and move individual objects in the scene. However, our aim is not to propose a superior method for nonprehensile manipulation, but rather to explore the capabilities and limitations of learning-based video prediction models for performing robotic control tasks from scratch, with minimal prior knowledge.

Our results, shown in Table I, indicate that our method is indeed able to leverage the predictive model to improve over the performance of the baselines. The performance of our method compared to the last two baselines suggests that our method is making meaningful inferences about the motion of objects in response to the arm. Although these results leave significant room for improvement, they suggest that predictive models can be used with minimal prior knowledge to perform robotic manipulation tasks. As video prediction models continue to improve, we expect that the performance of our method will improve with them. In the next section, we analyze specific physical interactions to better understand the capabilities and limitations of our model.

TABLE I

QUANTITATIVE COMPARISON: MEAN DISTANCE BETWEEN FINAL AND GOAL PIXEL POSITIONS

method	mean pixel distance
initial pixel position	5.10 ± 2.25
1) random actions	4.05 ± 1.75
2) move end-effector to goal	3.79 ± 2.66
3) move end-effector along vector (with replanning)	3.19 ± 1.68
visual MPC (ours)	$\mathbf{2.52 \pm 1.06}$

C. Qualitative Results

In this section, we evaluate the capabilities and limitations of visual MPC with a set of qualitative experiments. The goal of these experiments is to determine whether or not the model can perform more complex manipulations that require reasoning about object rotations and centers of mass. One of the benefits of planning actions with a predictive model of all pixels is that the model can be used to plan actions that affect multiple pixels, causing them to move in different directions in a coordinated fashion. For example, object rotation can be represented by moving the pixels on opposite ends of an object in opposite directions. To evaluate this capability, we command the robot to rotate objects by specifying opposing

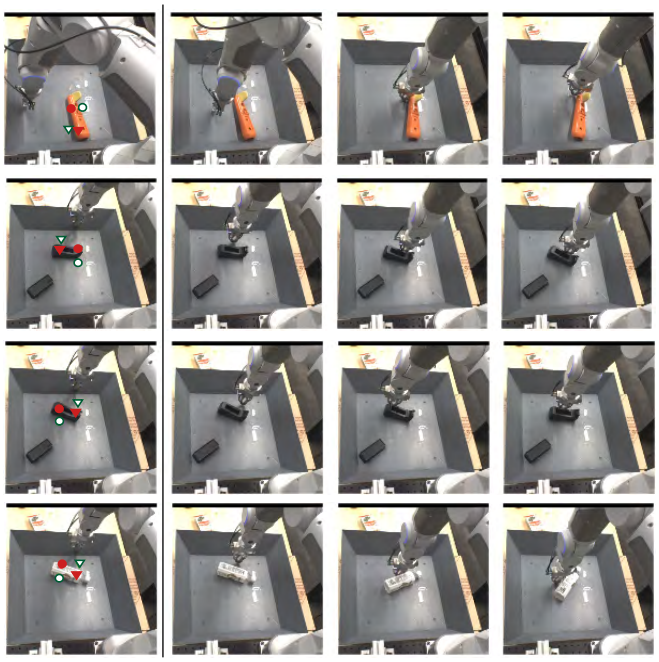

Fig. 5. When commanded to rotate objects by moving their end-points in opposing directions, our method plans for actions that touch the object on one side. In the initial image on the left, the red markers designate the user-specified starting pixel positions, and the green-outlined markers show the corresponding goal positions. Note that the arm starts some distance from the object, forcing the model to plan for the right contact position to realize the rotation. The black tape in the middle two rows was in the original dataset, while the other two objects were not.

motions for pixels on either extreme of the object, as shown on the left in Figure 5. When commanded to move pixels such that an object rotates, our method is able to produce the desired rotational motion, as seen on the right side of Figure 5. These examples indicate that the model can indeed be used for predicting the motion of multiple pixels and planning to affect them in a coordinated way.

One limitation of our approach is in handling self-occlusions. Once the arm occludes the object, the designated pixel is on the arm instead of the object, and the method subsequently plans to move the arm instead of the object into the goal position. An example of this failure case is shown in Figure 6. Incorrect model predictions also cause failures in performance. As shown in the second row of Figure 6, the robot selects a sequence of actions that push the bottle too close to its center of mass, causing it to translate rather than rotate. We expect that, by improving the accuracy of video prediction models, we can reduce such failures, and increase the general performance of the method. Video prediction is an active area of research in deep learning and computer vision [38], [43], [44] and, with the method described in this work, improvements to such predictive models could translate into improvements in robotic manipulation capabilities.

VI. Discussion & Future Work

We presented a learning-based approach for basic non-prehensile manipulation. Our method uses a deep predictive neural network model to plan pushing motions with minimal prior engineering. We use a convolutional LSTM model trained on unlabeled data collected autonomously by a team of robots. This model predicts future camera images and image-space pixel flow, conditioned on a sequence of motor commands. By inferring the commands that will move individual points in an image to desired target locations, we can continuously plan for pushing tasks even with novel objects not previously seen during training. Since the model is trained entirely through a self-supervised procedure, the method is well suited for continuous self-improvement through constant data collection. Our experimental evaluation demonstrates that our method outperforms simple baselines based on geometric heuristics and known hand-to-camera calibration.

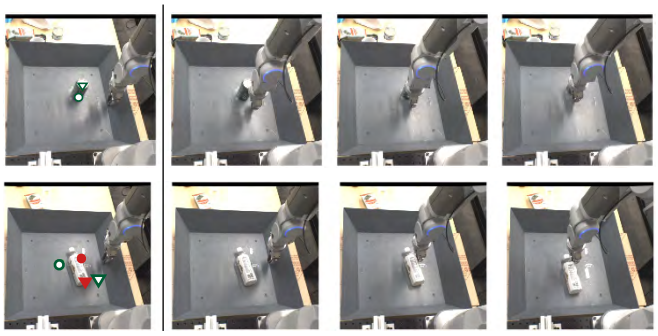

Fig. 6. Two failure cases of our method. In the first scenario, the goal is to avoid moving the can. The arm moves in front of the can, occluding it, causing the estimated pixel positions to shift, and causing the arm to later bump into the can. In the second example, the goal is to rotate the bottle. Although the robot makes contact with the bottle in a reasonable location to perform the rotation, it underestimates the mass of the bottle (which is empty). Instead of rotating, the light bottle simply translates along with the robot's arm.

Although we show generalization to completely novel objects, our model is still limited to relatively simple short-horizon tasks. As the accuracy of deep video prediction models improves, we expect the capabilities of this approach to also improve. Predictive models that estimate distributions over future images are particularly promising for robotic control, since planning under such models corresponds to maximum likelihood inference for determining a sequence of actions that maximizes the probability of the desired outcome. A promising direction for future work is to integrate the latest advances in such probabilistic video prediction models, e.g. [43], into our approach.

One of the enabling technologies for our approach is the available of fast, highly parallel GPUs for runtime evaluation of our model. All of our experiments use a commercially available GPU, which makes the approach practical for self-contained robotic systems. However, the planning horizon and replanning rate are limited by computational power, and the availability of even faster and more parallel computational platforms will likely lead to an improvement in capability and accuracy.

Finally, we believe that this work represents a relatively early first step toward model-based robotic control using

learned predictive models. Deep neural network-based video prediction is still in its early stages, with most state-of-the-art methods making accurate predictions only a few frames into the future [38]. As the state-of-the-art in video prediction improves, model-based methods will become increasingly more powerful. Of particular interest for robotic manipulation, hierarchical models operating at varying time scales [45] may even make it practical to plan highly elaborate skills entirely using learned predictive models.

REFERENCES

[1] C. Szegedy, S. Ioffe, and V. Vanhoucke, "Inception-v4, inception-resnet and the impact of residual connections on learning," *arXiv preprint arXiv:1602.07261*, 2016.

[2] J. Dai, Y. Li, K. He, and J. Sun, "R-fcn: Object detection via region-based fully convolutional networks," *arXiv preprint arXiv:1605.06409*, 2016.

[3] T. P. Lillicrap, J. J. Hunt, A. Pritzel, N. Heess, T. Erez, Y. Tassa, D. Silver, and D. Wierstra, "Continuous control with deep reinforcement learning," *International Conference on Learning Representations (ICLR)*, 2016.

[4] S. Levine, C. Finn, T. Darrell, and P. Abbeel, "End-to-end training of deep visuomotor policies," *Journal of Machine Learning Research (JMLR)*, 2016.

[5] V. Mnih, K. Kavukcuoglu, D. Silver, A. A. Rusu, J. Veness, M. G. Bellemare, A. Graves, M. Riedmiller, A. K. Fidjeland, G. Ostrovski *et al.*, "Human-level control through deep reinforcement learning," *Nature*, 2015.

[6] C. Finn, I. Goodfellow, and S. Levine, "Unsupervised learning for physical interaction through video prediction," in *Neural Information Processing Systems (NIPS)*, 2016.

[7] O. Khatib, "A unified approach for motion and force control of robot manipulators: The operational space formulation," *IEEE Journal on Robotics and Automation*, 1987.

[8] R. M. Murray, Z. Li, and S. S. Sastry, *A mathematical introduction to robotic manipulation*. CRC press, 1994.

[9] M. R. Dogar and S. S. Srinivasa, "A planning framework for non-prehensile manipulation under clutter and uncertainty," *Autonomous Robots*, 2012.

[10] M. Mason, "Mechanics and planning of manipulator pushing operations," *The International Journal of Robotics Research (IJRR)*, 1986.

[11] M. Salganicoff, G. Metta, A. Oddera, and G. Sandini, *A vision-based learning method for pushing manipulation*. AAAI Fall Symposium Series, 1993.

[12] A. Cosgun, T. Hermans, V. Emeli, and M. Stilman, "Push planning for object placement on cluttered table surfaces," in *International Conference on Intelligent Robots and Systems (IROS)*, 2011.

[13] K.-T. Yu, M. Bauza, N. Fazeli, and A. Rodriguez, "More than a million ways to be pushed: A high-fidelity experimental data set of planar pushing," *International Conference on Intelligent Robots and Systems (IROS)*, 2016.

[14] H. Murase and S. K. Nayar, "Visual learning and recognition of 3-d objects from appearance," *International Journal of Computer Vision (IJCV)*, 1995.

[15] A. Collet, D. Berenson, S. S. Srinivasa, and D. Ferguson, "Object recognition and full pose registration from a single image for robotic manipulation," in *International Conference on Robotics and Automation (ICRA)*, 2009.

[16] F. Endres, J. Trinkle, and W. Burgard, "Learning the dynamics of doors for robotic manipulation," in *International Conference on Intelligent Robots and Systems (IROS)*, 2013.

[17] P. McLeod, N. Reed, and Z. Dienes, "Psychophysics: How fielders arrive in time to catch the ball," *Nature*, 2003.

[18] D. Pomerleau, "Alvinn; an autonomous land vehicle in a neural network," *Neural Information Processing Systems (NIPS)*, 1989.

[19] R. Hadsell, P. Sermanet, J. Ben, A. Erkan, M. Scoffier, K. Kavukcuoglu, U. Muller, and Y. LeCun, "Learning long-range vision for autonomous off-road driving," *Journal of Field Robotics (JFR)*, 2009.

[20] M. Riedmiller, T. Gabel, R. Hafner, and S. Lange, "Reinforcement learning for robot soccer," *Autonomous Robots*, 2009.

[21] L. Pinto and A. Gupta, "Supersizing self-supervision: Learning to grasp from 50k tries and 700 robot hours," *International Conference on Robotics and Automation (ICRA)*, 2016.

[22] S. Levine, P. Pastor, A. Krizhevsky, and D. Quillen, "Learning hand-eye coordination for robotic grasping with deep learning and large-scale data collection," *International Symposium on Experimental Robotics (ISER)*, 2016.

[23] M. Deisenroth and C. E. Rasmussen, "Pilco: A model-based and data-efficient approach to policy search," in *International Conference on Machine Learning (ICML)*, 2011.

[24] P. Abbeel, A. Coates, M. Quigley, and A. Y. Ng, "An application of reinforcement learning to aerobatic helicopter flight," *Neural Information Processing Systems (NIPS)*, 2007.

[25] Y. Tassa, T. Erez, and E. Todorov, "Synthesis and stabilization of complex behaviors through online trajectory optimization," in *International Conference on Intelligent Robots and Systems (IROS)*, 2012.

[26] I. Lenz, R. Knepper, and A. Saxena, "Deepmpc: Learning deep latent features for model predictive control," in *Robotics Science and Systems (RSS)*, 2015.

[27] B. Boots, A. Byravan, and D. Fox, "Learning predictive models of a depth camera & manipulator from raw execution traces," in *International Conference on Robotics and Automation (ICRA)*, 2014.

[28] A. Byravan and D. Fox, "Se3-nets: Learning rigid body motion using deep neural networks," *arXiv preprint arXiv:1606.02378*, 2016.

[29] P. Agrawal, A. Nair, P. Abbeel, J. Malik, and S. Levine, "Learning to poke by poking: Experiential learning of intuitive physics," *Neural Information Processing Systems (NIPS)*, 2016.

[30] B. Boots, S. M. Siddiqi, and G. J. Gordon, "Closing the learning-planning loop with predictive state representations," *The International Journal of Robotics Research (IJRR)*, 2011.

[31] S. Lange, M. Riedmiller, and A. Voigtlander, "Autonomous reinforcement learning on raw visual input data in a real world application," in *International Joint Conference on Neural Networks (IJCNN)*, 2012.

[32] M. Watter, J. Springenberg, J. Boedecker, and M. Riedmiller, "Embed to control: A locally linear latent dynamics model for control from raw images," in *Neural Information Processing Systems (NIPS)*, 2015.

[33] C. Finn, X. Y. Tan, Y. Duan, T. Darrell, S. Levine, and P. Abbeel, "Deep spatial autoencoders for visuomotor learning," *International Conference on Robotics and Automation (ICRA)*, 2016.

[34] B. Espiau, F. Chaumette, and P. Rives, "A new approach to visual servoing in robotics," *IEEE Transactions on Robotics and Automation*, 1992.

[35] K. Mohta, V. Kumar, and K. Daniilidis, "Vision based control of a quadrotor for perching on planes and lines," in *International Conference on Robotics and Automation (ICRA)*, 2014.

[36] W. J. Wilson, C. W. W. Hulls, and G. S. Bell, "Relative end-effector control using cartesian position based visual servoing," *IEEE Transactions on Robotics and Automation*, 1996.

[37] A. Censi and R. M. Murray, "Bootstrapping bilinear models of Simple Vehicles," *International Journal of Robotics Research*, 2015.

[38] M. Mathieu, C. Couprie, and Y. LeCun, "Deep multi-scale video prediction beyond mean square error," *International Conference on Learning Representations (ICLR)*, 2016.

[39] D. P. Kingma and M. Welling, "Auto-encoding variational bayes," *International Conference on Learning Representations (ICLR)*, 2014.

[40] J. L. Ba, J. R. Kiros, and G. E. Hinton, "Layer normalization," *arXiv preprint arXiv:1607.06450*, 2016.

[41] R. Y. Rubinstein and D. P. Kroese, *The cross-entropy method: a unified approach to combinatorial optimization, Monte-Carlo simulation and machine learning*. Springer Science & Business Media, 2013.

[42] R. Anderson, D. Gallup, J. T. Barron, J. Kontkanen, N. Snavely, C. Hernández, S. Agarwal, and S. M. Seitz, "Jump: Virtual reality video," *SIGGRAPH Asia*, 2016.

[43] J. Walker, C. Doersch, A. Gupta, and M. Hebert, "An uncertain future: Forecasting from static images using variational autoencoders," *European Conference on Computer Vision (ECCV)*, 2016.

[44] W. Lotter, G. Kreiman, and D. Cox, "Deep predictive coding networks for video prediction and unsupervised learning," *arXiv preprint arXiv:1605.08104*, 2016.

[45] S. El Hihi and Y. Bengio, "Hierarchical recurrent neural networks for long-term dependencies." in *Neural Information Processing Systems (NIPS)*, 1995.